HHS Public Access

Author manuscript

J Allergy Clin Immunol. Author manuscript; available in PMC 2016 November 01.

Published in final edited form as:

J Allergy Clin Immunol. 2015 November ; 136(5): 1326–1336. doi:10.1016/j.jaci.2015.04.008.

Single-cell systems level analysis of human Toll-Like-Receptor activation defines a chemokine signature in Systemic Lupus Erythematosus

William E. O'Gorman, PhD[a,i,l], **Elena W.Y. Hsieh, MD**[a,b,i], **Erica S. Savig, BA**[c,j], **Pier Federico Gherardini, PhD**[a,j], **Joseph D. Hernandez, MD PhD**[b,d], **Leo Hansmann, PhD**[a], **Imelda M. Balboni, MD PhD**[b], **Paul J. Utz, MD PhD**[e,f], **Sean C. Bendall, PhD**[d], **Wendy J. Fantl, PhD**[a,g], **David B. Lewis, MD**[b], **Garry P. Nolan, PhD**[a,f,k,*], and **Mark M. Davis, PhD**[a,f,h,k,*]

[a]Department of Microbiology and Immunology, Stanford University, Stanford, CA 94305, USA

[b]Department of Pediatrics, Division of Allergy, Immunology and Rheumatology, Stanford University, Stanford, CA 94305, USA

[c]Cancer Biology Program, Stanford University, Stanford, CA 94305, USA

[d]Department of Pathology, Stanford University, Stanford, CA 94305, USA

[e]Department of Medicine, Division of Immunology and Rheumatology, Stanford University, Stanford, CA 94305, USA

[f]Institute for Immunity, Transplantation and Infection, Stanford University, Stanford, CA 94305, USA

[g]Department of Obstetrics and Gynecology, Division of Gynecologic Oncology, Stanford University, Stanford, CA 94305, USA

[h]The Howard Hughes Medical Institute, Stanford University, Stanford, CA 94305, USA

Abstract

[*]Correspondence: gnolan@stanford.edu (G.P.N.), mmdavis@stanford.edu (M.M.D.) Corresponding authors Garry P. Nolan, Ph.D. 269 Campus Drive, Ctr for Clinical Sciences Research 3205 Stanford, CA 94305-5175 Tel: (650) 725-7002 Fax: (650) 723-2383 Mark M. Davis, Ph.D. 279 Campus Drive, Beckman Center B221 Stanford, CA 94305-5175 Tel: (650) 725-4755 Fax: (650) 498-7771.

[i]Co-first authors

[j]Co-second authors

[k]Co-senior authors

[l]W.E.O. current affiliation: ITGR/OMNI Biomarkers, Development Sciences, Genentech, South San Francisco, CA94080

W.E.O, E.W.Y.H., G.P.N. and M.M.D. conceived the study. W.E.O. and E.W.Y.H. developed reagents, performed all data acquisition experiments, biological analysis, and data interpretation. E.S.S. developed the signaling network heatmap visualization tool. P.F.G. conceived and designed the monocyte cytokine combinatorial heatmap. J.D.H. assisted with manuscript writing. L.H. aided in healthy donor sample acquisition. E.W.Y.H. and I.M.B. recruited SLE patients and healthy controls. D.B.L., I.M.B. and P.J.U. provided intellectual guidance and expertise in immunobiology and autoimmunity. S.C.B. provided mass cytometry expertise. W.J.F. assisted with data interpretation and manuscript writing. W.E.O., E.W.H., G.P.N. and M.M.D wrote the manuscript.

Background—Activation of Toll-Like Receptors (TLRs) induces inflammatory responses involved in immunity to pathogens and autoimmune pathogenesis, such as in Systemic Lupus Erythematosus (SLE). Although TLRs are differentially expressed across the immune system, a comprehensive analysis of how multiple immune cell subsets respond in a system-wide manner has previously not been described.

Objective—To characterize TLR activation across multiple immune cell subsets and individuals, with the goal of establishing a reference framework against which to compare pathological processes.

Methods—Peripheral whole blood samples were stimulated with TLR ligands, and analyzed by mass cytometry simultaneously for surface marker expression, activation states of intracellular signaling proteins, and cytokine production. We developed a novel data visualization tool to provide an integrated view of TLR signaling networks with single-cell resolution. We studied seventeen healthy volunteer donors and eight newly diagnosed untreated SLE patients.

Results—Our data revealed the diversity of TLR-induced responses within cell types, with TLR ligand specificity. Subsets of NK and T cells selectively induced NF-κB in response to TLR2 ligands. CD14hi monocytes exhibited the most polyfunctional cytokine expression patterns, with over 80 distinct cytokine combinations. Monocytic TLR-induced cytokine patterns were shared amongst a group of healthy donors, with minimal intra- and inter- individual variability. Furthermore, autoimmune disease altered baseline cytokine production, as newly diagnosed untreated SLE patients shared a distinct monocytic chemokine signature, despite clinical heterogeneity.

Conclusion—Mass cytometry analysis defined a systems-level reference framework for human TLR activation, which can be applied to study perturbations in inflammatory disease, such as SLE.

Keywords

Mass cytometry; Toll-Like-Receptors; systemic lupus erythematosus; inflammation; monocytes; MCP1

INTRODUCTION

Pattern Recognition Receptors (PRRs) recognize conserved features of foreign microorganisms during infection, and self-molecules in tissue injury[1,2]. Toll-like receptors (TLRs) were the first identified family of PRRs; the human genome encodes ten TLRs[3,4]. TLRs are type 1 transmembrane receptors with an extracellular ligand-binding domain, a transmembrane domain, and a cytoplasmic Toll/IL-1R (TIR) domain[3,5]. TLRs are expressed on the plasma membrane (TLRs 1, 2, 4, 5, 6) or in endosomes (TLRs 3, 7, 8, 9)[6]. Ligand binding to TLRs induces dimerization of the TIR domains. This dimer functions as a scaffold for MyD88 or TRIF protein adaptor complexes, which then activate MAPK and NF-κB pathways, or IRFs, respectively[7,8]. Crosstalk with other pathways elicits the production of inflammatory and regulatory cytokines that shape adaptive immunity[9]. Although TLR-induced inflammation is important for antimicrobial responses, inappropriate TLR recognition of self-molecules results in the development of autoimmune diseases such as Systemic Lupus Erythematosus (SLE)[10,11]. In SLE, self-nucleic acid containing

antibodies form immune complexes that can sequentially activate Fcγ and endosomal TLR receptors[12-14].

To maintain the balance between protective immunity and inflammatory disease, TLR signaling and cytokine production are precisely regulated at multiple levels. First, the cellular compartmentalization of TLRs limits their accessibility to ligands. Second, different immune cell populations selectively express certain TLRs and TLR-inducible signaling pathways[15]. Finally, each immune cell subset produces a distinct set of cytokines. Systems-scale proteomic approaches have previously been applied to characterize this level of complexity of TLR networks. For example, mass-spectrometry based phosphoproteome analysis was used to profile TLR-induced signaling in murine macrophages[16,17]. A separate study applied mass-spectrometry based secretomic analysis to evaluate cytokine production elicited by TLR activation in murine macrophages and dendritic cells[18,19]. These studies, while informative, have provided global views of TLR signaling and cytokine production in specific immune cell subsets, but not within the context of an integrated cellular immune system with single-cell resolution.

To achieve a systems-level perspective of TLR biology that simultaneously accounts for functional diversity at the single-cell level, the activation of intracellular signaling pathways, and cytokine production, we capitalized on the ability of mass cytometry to capture this complexity. Here, 40-parameter mass cytometry was used to define a reference framework for human TLR activation *ex vivo* in whole blood samples. The application of this framework to evaluate cytokine alterations in a systemic inflammatory disease such as SLE revealed a characteristic abnormal monocytic chemokine signature in SLE patients in the basal state, in the absence of any *ex vivo* stimulation. This study demonstrates the utility of this approach to characterize TLR activation across the immune system and in inflammatory diseases in general.

METHODS

Study participants

All human donors were enrolled under a study protocol approved by the Institutional Review Board of the Research Compliance Office at Stanford University. Written informed consent was obtained from all study participants. Inclusion/exclusion criteria for healthy volunteer donors and SLE patients found in supplementary methods (**Table E1**). SLE patients fulfilled the revised American College of Rheumatology (ACR) diagnostic criteria[20] (**Table E2**).

Sample processing, stimulation, and cytometry analysis

Donor whole blood was collected into heparinized vacutainers (BD), incubated at 37°C with TLR ligands (**Table E4**), fixed and permeabilized for intracellular staining. Conditions for signaling proteins and intracellular cytokine staining were adapted from previous studies[21,22] (supplementary methods). Clone, vendor, and conjugation information for all monoclonal antibodies are shown in **Table E3**. Cells were analyzed on a CyTOF®

instrument (Fluidigm); data were acquired using internal metal isotope bead standards, normalized, and analyzed as previously described[23,24] (Flowjo Treestar and Cytobank).

"Signaling network heatmap" visualization tool

In brief, for each experimental condition and cell type population, representative single-cells were sampled and ordered from lowest to highest transformed value for each signaling proteins. Subtractions between stimulated and unstimulated conditions yielded single-cell signaling fold changes, which were colored and packed together into a "signaling node." See supplementary methods for data processing steps and visualization development.

CD14hi monocytes combinatorial cytokine heatmap

In brief, cytokine positivity was determined in a binary fashion based on 95th percentile intensity threshold; CD14hi monocyte subpopulations expressing different cytokine combinations were clustered based on similar cytokine response profiles induced by TLR ligands. See supplementary methods for data processing and computational design.

Statistical analysis of CD14hi monocyte cytokine signatures

Comparison of the mean percent positivity (defined by 95th percentile threshold as above) for each monocytic cytokine, between the SLE and healthy control groups, was performed by applying a Student's t-test, with Bonferroni adjustment, which apportions the significance level evenly among the nine hypothesis tests (p-value=0.0056 adjusted significance level, Microsoft Excel 2011).

RESULTS

Mass cytometry identifies major immune cell subsets in human whole blood

Using *a priori* knowledge about hematopoietic lineages, human blood cells were categorized into 11 major immune cell subsets (**Figures 1, E1**). Granulocytes, B cells, and T cells were classified based on surface marker expression of CD66, CD19/CD20/HLADR, and CD3, respectively[21]. CD3-/CD19-/HLADR-/CD7+ lymphocytes[25] were subdivided into CD16hi and CD56hi subsets[26] NK cell subsets. CD11c and HLADR co-expression defined nongranulocytic myeloid cells[27]. CD11clo/HLADRhi/CD123+ cells were classified as plasmacytoid dendritic cells (pDCs)[28]. CD11c+/HLADR+ monocytes were subdivided into CD14hi (classical) and CD16hi (non-classical) subsets[29]. CD1c expression defined conventional dendritic cells (CD1c+ DCs)[27], and FcεRI and CD123 co-expression identified basophils[30]. TLRs, their ligands, signaling pathways and cytokines examined are listed in **Figure 1**.

A "signaling network heatmap" visualization tool provides an integrated view of TLR signaling patterns

Changes in the activation states of nine signaling proteins were monitored in eleven cell subsets, in response to eight stimuli. Conventional depiction of such high-density data with 2D plots, histograms, or heatmaps does not capture an integrated view of all the measured parameters, nor does it make the most of the single-cell resolution. To overcome this

analytical challenge, a “signaling network heatmap” visualization tool was developed. In brief, up to 1,000 representative single cells were sampled from each immune cell subset and TLR stimuli condition. For each cell type and condition, cells were ordered by expression value for every signaling protein, indexed from lowest to highest arcsinh transformed value. Arcsinh scale, a bioexponential transformation used in flow cytometry data, was chosen over traditional log scale to account for negative values[31]. For each cell type and signaling protein, expression values for that signaling protein in the stimulated and unstimulated conditions were paired according to their indexed transformed value. Differences between these paired values resulted in single-cell signaling fold changes (**Figure 2A**), which were colored according to the arcsinh difference (**Figure 2B**), and arranged into a “signaling node” (**Figure 2C**), based on their original index position. These signaling nodes were then arranged into pathways downstream of MyD88 and TRIF adaptor protein complexes (**Figure 2D**). The generalized pathways include NF-κB and AP-1 activation, as well as proteins involved in downstream transcriptional and translational regulation (further details in supplementary methods). Signaling network heatmap and variance data from other donors are shown in **Figures E2** and **E3**, respectively.

Systems level TLR signaling analysis demonstrates diverse signaling responses in myeloid cell subsets, and selective NF-κB activation in NK and T cell subsets

In the myeloid lineage, the induction of every measured signaling protein was observed in >95% of CD14hi and CD16hi monocytes, in response to all extracellular TLR ligands and the endosomal TLR7/8 ligand, R848 (15 to 100-fold increases, with the marginal activation of pERK, **Figure 2E**). Although pDCs only responded to endosomal stimuli, CD1c+ DCs TLR signaling responses largely overlapped with monocytic ones, with the exception of zymosan. Zymosan induced IκBα degradation in both CD1c+ DCs and CD14hi monocytes. However, zymosan also activated multiple other signaling pathways in CD14hi monocytes. This difference is potentially due to the fact that CD1c+ DCs express TLR2 only, while CD14hi monocytes express both TLR2 and dectin-1 receptors[32]. Like CD1c+ DCs, granulocytes responded to all extracellular ligands and R848 (**Figure 2E**). In contrast, only a fraction of basophils responded to PAM2 (TLR2/6 ligand; 15.5% responders) and to LPS (TLR4 ligand; 7.2% responders) with induction of IκBα degradation and p38 phosphorylation (**Figure 2E**). This restricted basophil signaling profile is concordant with previous studies on the roles of TLR2- and TLR4-mediated basophil activation in augmenting allergic reactions[33].

In the lymphoid lineage, endosomal TLR agonists induced NF-κB and CREB pathways in B cells (**Figures 3A, E4**). Unexpectedly, TLR2 ligands PAM2 (TLR2/6) and PAM3 (TLR1/2) selectively activated the NF-κB pathway in NK and T cell subsets (**Figure 3B, 3C**). In approximately one third of CD56hi NK cells, IκBα degradation (36.6% responders) was observed in response to PAM2 stimulation (also phosphorylation of pCREB and p38, **Figure E5A**). A lower frequency of CD56hi NK cells (20.1%) responded to PAM3 stimulation (**Figure E5A**). These responses were far less apparent in CD16hi NK cells (**Figures 3B, E5B**). To assess the reproducibility of this observation, PAM2 and PAM3 stimulations were performed in ten additional donor blood samples, resulting in IκBα degradation in 36% (SD=12.67%) and 24.3% (SD=17%) of CD56hi NK cells, respectively

(**Figure E5B**). To understand this further, NK cells were enriched to ~96.75% purity (supplementary methods) and stimulated with PAM2 and PAM3. IκBα degradation was mainly observed in the CD56hi NK population in response to PAM2, suggesting that this TLR ligand directly activated these cells (**Figure E6**).

As observed for NK cells, PAM2 and PAM3 stimulation also activated the NF-κB pathway in CD4 T cells (**Figure 3C**). This activity was even less apparent in CD8 T cells (**Figures 3C, E7A**). In a group of ten additional donors, an average of 14.5% (SD=5.1%) and 11.9% (SD=7.8%) CD4 T cells responded to PAM2 and PAM3, respectively (**Figure E7B**). To investigate whether PAM2 and PAM3 directly activated T cells, T cells enriched to ~96% purity were stimulated with these ligands and exclusive NF-κB pathway induction was observed in similar percentages of cells (average=14.03% and SD=5.1% for PAM2, average=4.32% and SD=5.1% for PAM3; **Figure E7C**), indicating that these lipopeptides are acting directly on T lymphocytes. Alhough previous studies have explored the role of TLR2 agonists in T cell activation[34,35], the activation of specific signaling pathways has not been well defined.

TLR-induced cytokine signatures demonstrate cell type and TLR ligand specificity

The production of 16 cytokines downstream of the signaling pathways examined above was simultaneously measured in myeloid and lymphoid cell types (**Figure 1** tables). Cytokine data was analyzed using a Boolean gating strategy, with positivity defined in **Figure E8**. TLR stimulation induced the production of 10 out of 16 cytokines in one or more myeloid cell populations, with minimal cytokine production in lymphoid cells (**Figures 4, E9**).

Mirroring TLR-induced signaling patterns, CD14hi monocyte and CD1c+ DC cytokine response profiles also largely overlapped (**Figures 4, E10**). However, CD1c+ DCs consistently produced more IL-12 (35.7% more, averaged over all TLR ligand conditions) after stimulation than did CD14hi monocytes (**Figure E10**). LPS and R848 induced different chemokine responses in CD14hi monocytes—LPS elicited IL-8 production in the absence of MCP1 expression, whereas R848 induced the converse (**Figure 4**). CD16hi monocytes were not included in the cytokine analysis because after 6-hour stimulation period, CD16 was shed from non-classical monocytes.

Unlike monocytes and CD1c+ DCs, pDCs demonstrated a restricted cytokine response repertoire, primarily IFNα production in response to endosomal TLR agonists (**Figure 4**). Granulocytes and basophils produced MiP1β, IL-8, and IL-1RA only (**Figure E9A**). Minimal cytokine production was observed in the lymphoid compartment (**Figure E9B**), even for B cells, in which endosomal TLR stimulation induced signaling responses (**Figures 3A**). Despite the PAM2- and PAM3-driven NF-κB signaling activation observed in NK and T cell subpopulations (**Figure 3B, 3C**), cytokine responses were not induced in these cells (**Figure E9B**), suggesting that these TLR ligands play a co-stimulatory role in antigen receptor activation.

TLR ligands induce diverse combinatorial cytokine signatures in CD14hi monocytes

Combinatorial cytokine production is the ability to produce numerous combinations of cytokines simultaneously. T cells have been shown to exhibit combinatorial polyfunctional cytokine responses that are correlated with resistance to disease[36,37]. It is not clear, however, whether myeloid cell populations share this capability. In this study, CD14hi monocytes produced the most diverse cytokine responses to TLR stimulation (**Figures 4, E10**). To emphasize salient polyfunctional combinations, only subsets with a minimum 1% population frequency were included in the analysis. Here, we found that 83 out of the possible 512 combinations meet that threshold (**Figure 5)**. Hierarchical clustering of these cytokines into a combinatorial heatmap exposed relationships between cytokines that are co-expressed (**Figure 5**, left panel) and between TLR stimuli that elicit similar cytokine responses (**Figure 5**, right panel). IL-1β and Mip1β behaved the most similarly, and pro-inflammatory cytokines IL-12 and TNFα formed a separate cluster.

PAM2, PAM3, and flagellin elicited similar cytokine profiles; generally, two or three cytokines were expressed, primarily IL-1β, Mip1β, and IL-8 (**Figure 5**, right panel). LPS and zymosan also induced similar combinatorial cytokine signatures, likely related to the synergistic effects of dectin-1 with TLR2 and TLR4[32]. R848 and LPS induced comparable monocytic polyfunctionality (**Figure 5**, right panel), but differed in the type of cytokines induced (**Figure 5**, left panel). These cytokine combinatorial phenotypes suggest a monocytic functional specialization that cannot be defined by surface marker-based classifications alone.

CD14hi monocytes from SLE patients show an inflammatory cytokine signature typified by MCP1

To assess the reproducibility of this approach for evaluating TLR-induced cytokine production, the intra- and inter-individual variability in healthy donors were determined. Monocytic TLR-induced cytokine patterns were highly conserved over time for a single donor (**Figure 6A**) and amongst nine healthy donors (**Figure 6B**). The least degree of intra- and inter-individual variability was observed for Mip1β production with standard deviation ranging from 1.02% (LPS) to 5.25% (R848) for one donor over time, and 0.41% (R848) to 4.44% (LPS) amongst nine donors (**Figure E11**). IL-12 production varied most with a standard deviation of 13.3% for one donor longitudinally, and 18.2% for nine donors, in the R848 condition (**Figure E11**). These results demonstrate the reproducibility of this experimental platform, and validate the data as a reference framework of TLR-induced cytokine profiles in healthy donors. This reference framework was used to compare cytokine profiles in an inflammatory disease in which abnormal TLR responses drive pathological cytokine production, such as SLE[38,39].

Analysis of blood samples from eight newly diagnosed, untreated, and clinically heterogeneous SLE patients (**Table E2**) revealed a common abnormal CD14hi monocytic cytokine signature in the basal state, in the absence of *ex vivo* stimulation (**Figure 7**). To internally control these experiments, 95th percentile baseline thresholds (**Figure E7**) for all cytokines were defined based on an initial time point when blood was immediately processed after draw (time zero) (**Figure E10**). CD14hi monocytes from each of the eight

newly diagnosed untreated SLE patients exhibited elevated levels of MCP1 (average=82.6%, SD=9.7%, **Figure E8**) after six hours of secretion block in the absence of any stimulation. Under these conditions, levels of MCP1 in corresponding healthy controls (different healthy donors than those in **Figure 6**) did not change to the same extent (average=18.8%, SD=8.1%, **Figure E12**). MCP1 is an inducible pro-inflammatory chemokine involved in the immunopathogenesis of human and murine lupus nephritis[40]. In murine SLE models, MCP1 inhibition ameliorates lupus nephritis[41]. Previous studies and our data indicate that MCP1 holds promise as a therapeutic target[41-44].

Levels of other cytokines such as Mip1β and TNFα were also elevated in newly diagnosed untreated SLE patient samples compared to those in healthy donor samples (**Figures 7, E13**). Bonferroni adjusted t-test calculation comparing average expression of each cytokine between the SLE patient and healthy control groups confirmed statistically significant differences in MCP1 (p-value=$7.6E^{-10}$), Mip1β (p-value=0.002), and TNFα (p-value=0.001). Comparison of cytokine profiles for all 11 cell subsets (as in **Figure 1**), for all eight SLE versus healthy matched-control pairs, did not demonstrate any statistically significant differences other than those observed in CD14hi monocytes (data not shown). Although all samples from SLE patients demonstrated this common monocytic cytokine signature (MCP1, Mip1β, and TNFα) based on single cytokine positivity (**Figure 7**), patient combinatorial cytokine profiles differed (**Figure E14**).

In this study, using a systems-scale single-cell proteomic approach to characterize human TLR signaling and cytokine networks, we defined a reference framework that can be applied to study alterations in these parameters in inflammatory disease.

DISCUSSION

TLRs (and other PRRs) are involved in the complex balance between protective immunity and inflammatory disease. To elucidate how TLR networks calibrate innate and adaptive immune responses to maintain this balance, we have used high-dimensional mass cytometry to broadly measure intracellular signaling responses and cytokine profiles in healthy individuals and newly diagnosed untreated SLE patients.

This comprehensive TLR activation analysis in healthy individuals corroborates previous findings in TLR biology and reveals novel TLR signaling responses in NK and T cells. In order to depict these TLR-induced signaling patterns with single-cell resolution, a signaling network heatmap visualization tool (**Figure 2A-D**) was developed. This method enables the display the activation characteristics of nine signaling proteins in eleven cell subsets in response to eight TLR ligands, with over six hundred features and approximately 2 million data points in **Figure 2E**. This is a scalable tool to visualize high-dimensional datasets, and provides a framework through which the signaling biology of entire receptor systems can be explored with nearly single-cell resolution.

While TLR responses have been extensively investigated in myeloid cells, they are not well defined in the lymphoid lineage, with the exception of B cells[45]. In our analysis, only TLR2 and TLR5 ligands activated signaling, primarily in CD56hi NK cells (**Figure 3B**). TLR2-

dependent NK cell activation has been linked to poxvirus and mycobacterial immunity[46,47]. Notably, TLR2-mediated mycobacterial recognition promotes NK-DC cross talk and IL-12 production [48], but it is unclear whether TLR2 stimuli directly activated NK cells. It is unlikely that the observed signaling responses (**Figures 2E, 3**) were indirect (paracrine) in nature, given 30-minute incubation; however, indirect effects cannot be completely excluded. Therefore, purified cell populations were assayed to evaluate non-canonical TLR ligand responses in NK and T cells. Here, we found that an enriched NK cell population responded to TLR2 ligands within 30 minutes, showing that NK cells can directly respond to these ligands (**Figure E6**).

Similarly, TLR responses in T cells are also poorly described. A subset of CD4 T cells degraded IκBα following TLR2 stimulation (**Figure 3C**), but this did not lead to cytokine production (**Figure E9B**). This pathway selectivity and the inability of TLR2 ligands alone to induce cytokine production in T cells suggest a co-stimulatory role for TLR2 in T cell activation. This observation is consistent with, and may provide a molecular mechanism for, previous reports that mycobacterial ligands and the live Bacillus Calmette-Guerin vaccine enhance T cell proliferation and cytokine production only when coupled with T cell receptor engagement[35,49]. These results also suggest that microbial lipopeptides should be explored as adjuvants in vaccine design. Detailed NK and T cell phenotyping could be incorporated in future studies to further understand this isolated signaling response to TLR2 ligands.

TLR activation was tracked from signal transduction to cytokine production, demonstrating how different TLR agonists elicited distinct cytokine combinations across the immune system. In order to construct a systems-level TLR activation reference framework, we compared TLR-induced cytokine responses longitudinally in a single donor and amongst healthy donors. Minimal intra- and inter-individual variability (**Figure 6**) suggested the applicability of this framework to study an inflammatory disease such as SLE. Compared to monocytes from healthy controls, CD14hi monocytes from eight newly diagnosed untreated SLE patients exhibited a statistically significant distinct cytokine signature (MCP1, Mip1β, and TNFα) at basal state, with the most prominent and uniform of the cytokines being MCP1 (**Figures 7, E13**). These eight SLE patients manifested diverse clinical symptoms (**Table E2**), which is characteristic of this complex autoimmune disorder. Yet, significantly, using our analysis system they all expressed this cytokine signature, particularly MCP1, suggesting that they shared an underlying basis that could be useful in both diagnosis and treatment. Additionally, these patient samples were obtained prior to any immunomodulatory treatment, thus there was no heterogeneity introduced by drug treatments.

MCP1 (also known as CCL2) recruits monocytes and lymphocytes to sites of inflammation[44]. Elevated MCP1 levels have been detected in a variety of autoimmune disorders[50-52], and often correlate with disease activity[42,44,53]. MCP1 may play a critical role in autoimmune end-organ damage, and MCP1 neutralization has been shown to ameliorate disease in rodent models of SLE[41]. The mechanism responsible for increased MCP1 production in SLE is unclear, but available data suggest several possibilities. First, MCP1 is a known type I IFN inducible chemokine[54]. Multiple transcriptomic studies have observed an IFNα signature in SLE patients, likely induced by nucleic acid containing

immune complexes activating endosomal TLRs in pDCs [12,55] and possibly leading to MCP1 induction. Second, Fcγ receptor activation elicits monocytic MCP1 production[56], and thus circulating immune complexes in SLE patients could explain MCP1 induction[14]. Finally, although RNA-containing immune complexes in SLE patients may activate TLR8 in monocytes leading to MCP1 production, monocytic cytokine profiles from SLE patients did not match R848-induced cytokine profiles, making this explanation unlikely. Regardless of the etiology of MCP1 production, MCP1 neutralization could potentially serve as an anti-inflammatory adjunctive therapy to reduce the usage or dosage of cytotoxic immunosuppressive drug regimens that are necessary to control SLE.

In conclusion, mass cytometry was utilized to generate a comprehensive reference framework of human TLR-driven immune responses in myeloid and lymphoid lineages. Analysis of SLE patient samples demonstrated that this reference framework could be applied to study inflammatory disease. Additionally, this study establishes a paradigm for using high-dimensional single-cell proteomic approaches to generate reference maps of other receptor systems.

Supplementary Material

Refer to Web version on PubMed Central for supplementary material.

ACKNOWLEDGEMENTS

We would like to thank Zachary B. Bjornson, Monica Nicolau, Nima Aghaeepour, Tiffany J. Chen, and Karen Sachs for their assistance in data analysis. We thank John S. Tamaresis and Karen Sachs for their assistance with statistical analysis, and Cristina Tato for helpful discussions. We thank Michael D. Leipold from the Human Immune Monitoring Core (HIMC), Angelica Trejo and Astraea Jager for their intellectual and technical contributions. E.W.Y.H. is a fellow of the Pediatric Scientist Development Program. She is supported by award number K12-HD000850 from the *Eunice Kennedy Shriver* National Institute of Child Health and Human Development, the Lucile Packard Foundation for Children's Health, Stanford CTSA UL1 TR001085, and Child Health Research Institute of Stanford University. E.S.S. is a National Science Foundation Graduate Research Fellow and Gabilon Stanford Graduate Research Fellow. P.F.G. is a Howard Hughes Medical Institute Fellow of the Life Sciences Research Foundation. J.D.H. is funded by the American Academy of Allergy, Asthma and Immunology Mylan Anaphylaxis Research Award. I.M.B. is supported by the NIH grant K08 AI080945, the Stanford Child Health Research Institute, and the Arthritis Foundation Postdoctoral Fellowship. D.B.L. is supported by funds from NIH grants R01 AI083757 and R01 AI100121. S.C.B. is supported by the Damon Runyon Cancer Research Foundation Fellowship (DRG-2017-09) and the NIH R00 GM104148-03. This work is supported by funds from NIH grants U19AI057229, U19AI090019, U54CA149145, T32AI007290, N01HV00242, 1U19AI100627, 5R01AI07372405, R01CA184968, 1R33CA183654, R33CA183692; NIH-Baylor Research Institute 41000411217; NIH-Northrop Grumman Corp 7500108142; California Institute for Regenerative Medicine DR101477; Food and Drug Administration HHSF223201210194C; Bill and Melinda Gates Foundation OPP 1017093; the European Commission HEALTH.2010.1.2-1; Alliance for Lupus Research; Entertainment and Industry Foundation NWCRA grant; the U.S. Department of Defense OC110674, 11491122; and Howard Hughes Medical Institute. Funding sources had no involvement in study design, collection, analysis or interpretation of data; in writing, or in the decision to submit the article for publication.

ABBREVIATIONS

Myd88	Myeloid differentiation primary response gene 88
TRIF	TIR-domain-containing adapter-inducing interferon β
MAPK	Mitogen-activated protein kinase
NF-κB	Nuclear factor kappa-light-chain-enhancer of activated B cells

TBK1	TANK binding kinase 1
IRF	interferon regulatory factor
IKBα	nuclear factor of kappa light polypeptide gene enhancer in B-cells inhibitor α
S6	ribosomal S6 kinase
ERK	Extracellular signal regulated kinase
CREB	cAMP response element-binding protein
PAM2	PAM2CSK4
PAM3	PAM3CSK4
ODN	oligodeoxynucleotide
LPS	lipopolysaccharide
R848	Resiquimod
R837	Imiquimod
MCP1	Monocyte chemotactic protein 1
Mip1β	Macrophage inflammatory protein 1β
TNFα	Tumor necrosis factor α
IFNα	Interferon α

REFERENCES

1. Ishii KJ, Koyama S, Nakagawa A, Coban C, Akira S. Host Innate Immune Receptors and Beyond: Making Sense of Microbial Infections. Cell Host & Microbe. 2008; 3:352–63. [PubMed: 18541212]
2. Akira S, Umeatsu S, Takeuchi O. Pathogen Recognition and Innate Immunity. Cell. 2006; 124:783–801. Available from. [PubMed: 16497588]
3. Netea MG, Wijmenga C, O'Neill LAJ. Genetic variation in Toll-like receptors and disease susceptibility. Nature Immunology. 2012; 13:535–42. [PubMed: 22610250]
4. O'Neill LAJ, Golenbock D, Bowie AG. The history of Toll-like receptors — redefining innate immunity. Nat Rev Immunol. 2013; 13:453–60. [PubMed: 23681101]
5. Beutler B, Eidenschenk C, Crozat K, Imler J-L, Takeuchi O, Hoffmann JA, et al. Genetic analysis of resistance to viral infection. Nat Rev Immunol. 2007; 7:753–66. [PubMed: 17893693]
6. Blasius AL, Beutler B. Intracellular Toll-like Receptors. Immunity. 2010; 32:305–15. [PubMed: 20346772]
7. Takeuchi O, Akira S. Pattern Recognition Receptors and Inflammation. Cell. 2011; 140:805–20. [PubMed: 20303872]
8. Fitzgerald KA, Chen ZJ. Sorting out Toll Signals. Cell. 2006; 125:834–6. [PubMed: 16751092]
9. Iwasaki A, Medzhitov R. Regulation of adaptive immunity by the innate immune system. Science. 2010; 327:291–5. [PubMed: 20075244]
10. Theofilopoulos AN, Gonzalez-Quintial R, Lawson BR, Koh YT, Stern ME, Kono DH, et al. Sensors of the innate immune system: their link to rheumatic diseases. Nature Reviews Rheumatology. 2010; 6:146–56. [PubMed: 20142813]
11. Kawasaki T, Kawai T, Akira S. Recognition of nucleic acids by pattern-recognition receptors and its relevance in autoimmunity. Immunol Rev. 2011; 243:61–73. [PubMed: 21884167]

12. Ronnblom L, Pascual V. The innate immune system in SLE: type I interferons and dendritic cells. Lupus. 2008; 17:394–9. [PubMed: 18490415]
13. Pascual V, Farkas L, Banchereau J. Systemic lupus erythematosus: all roads lead to type I interferons. Current Opinion in Immunology. 2006; 18:676–82. [PubMed: 17011763]
14. Means TK, Latz E, Hayashi F, Murali MR, Golenbock DT, Luster AD. Human lupus autoantibody–DNA complexes activate DCs through cooperation of CD32 and TLR9. J Clin Invest. 2005; 115:407–17. [PubMed: 15668740]
15. Kawai T, Akira S. The role of pattern-recognition receptors in innate immunity: update on Toll-like receptors. Nature Immunology. 2010; 11:373–84. [PubMed: 20404851]
16. Weintz G, Olsen JV, hauf KFU, Niedzielska M, Amit I, Jantsch J, et al. The phosphoproteome of toll-like receptor-activated macrophages. Molecular Systems Biology. 2010; 6:1–16.
17. Sjoelund V, Smelkinson M, Nita-Lazar A. Phosphoproteome Profiling of the Macrophage Response to Different Toll-Like Receptor Ligands Identifies Differences in Global Phosphorylation Dynamics. J Proteome Res. 2014; 13:5185–97. [PubMed: 24941444]
18. Luber CA, Cox J, Lauterbach H, Fancke Ben, Selbach M, Tschopp J, et al. Quantitative Proteomics Reveals Subset-Specific Viral Recognition in Dendritic Cells. Immunity. 2010:1–11.
19. Meissner F, Scheltema RA, Mollenkopf HJ, Mann M. Direct Proteomic Quantification of the Secretome of Activated Immune Cells. Science. 2013; 340:475–8. [PubMed: 23620052]
20. Yu C, Gershwin ME, Chang C. Diagnostic criteria for systemic lupus erythematosus: A critical review. Journal of Autoimmunity. 2014; 48-49:10–3. [PubMed: 24461385]
21. Jansen K, Blimkie D, Furlong J, Hajjar A, Rein-Weston A, Crabtree J, et al. Polychromatic flow cytometric high-throughput assay to analyze the innate immune response to Toll-like receptor stimulation. Journal of Immunological Methods. 2008; 336:183–92. [PubMed: 18565537]
22. Corbett NP, Blimkie D, Ho KC, Cai B, Sutherland DP, Kallos A, et al. Ontogeny of Toll-Like Receptor Mediated Cytokine Responses of Human Blood Mononuclear Cells. PLoS ONE. 2010; 5:e15041. [PubMed: 21152080]
23. Finck R, Simonds EF, Jager A, Krishnaswamy S, Sachs K, Fantl W, et al. Normalization of mass cytometry data with bead standards. Cytometry. 2013; 83A:483–94. [PubMed: 23512433]
24. Bendall SC, Simonds EF, Qiu P, Amir EAD, Krutzik PO, Finck R, et al. Single-Cell Mass Cytometry of Differential Immune and Drug Responses Across a Human Hematopoietic Continuum. Science. 2011; 332:687–96. [PubMed: 21551058]
25. Milush JM, Long BR, Snyder-Cappione JE, Cappione AJ, York VA, Ndhlovu LC, et al. Functionally distinct subsets of human NK cells and monocyte/DC-like cells identified by coexpression of CD56, CD7, and CD4. Blood. 2009; 114:4823–31. [PubMed: 19805616]
26. Poli A, Michel T, Thérésine M, Andrès E, Hentges F, Zimmer J. CD56 brightnatural killer (NK) cells: an important NK cell subset. Immunology. 2009; 126:458–65. [PubMed: 19278419]
27. Dzionek A, Fuchs A, Schmidt P, Cremer S, Zysk M, Miltenyi S, et al. BDCA-2, BDCA-3, and BDCA-4: three markers for distinct subsets of dendritic cells in human peripheral blood. J Immunol. 2000; 165:6037–46. [PubMed: 11086035]
28. Liu Y- J. IPC: Professional Type 1 Interferon-Producing Cells and Plasmacytoid Dendritic Cell Precursors. Annu Rev Immunol. 2005; 23:275–306. [PubMed: 15771572]
29. Ziegler-Heitbrock L, Ancuta P, Crowe S, Dalod M, Grau V, Hart DN, et al. Nomenclature of monocytes and dendritic cells in blood. Blood. 2010; 116:e74–e80. [PubMed: 20628149]
30. Hausmann OV, Gentinetta T, Fux M, Ducrest S, Pichler WJ, Dahinden CA. Robust expression of CCR3 as a single basophil selection marker in flow cytometry. Allergy. 2010; 66:85–91. [PubMed: 20608915]
31. Finak G, Perez J- M, Weng A, Gottardo R. Optimizing transformations for automated, high throughput analysis of flow cytometry data. BMC Bioinformatics. 2010; 11:546. [PubMed: 21050468]
32. Ferwerda G, Meyer-Wentrup F, Kullberg B- J, Netea MG, Adema GJ. Dectin-1 synergizes with TLR2 and TLR4 for cytokine production in human primary monocytes and macrophages. Cellular Microbiology. 2008; 10:2058–66. [PubMed: 18549457]

33. Bieneman AP, Chichester KL, Chen Y- H, Schroeder JT. Toll-like receptor 2 ligands activate human basophils for both IgE-dependent and IgE-independent secretion. Journal of Allergy and Clinical Immunology. 2005; 115:295–301. [PubMed: 15696084]
34. Sieling PA, Hill PJ, Dobos KM, Brookman K, Kuhlman AM, Fabri M, et al. Conserved mycobacterial lipoglycoproteins activate TLR2 but also require glycosylation for MHC class II-restricted T cell activation. J Immunol. 2008; 180:5833–42. [PubMed: 18424702]
35. Chen Q, Davidson TS, Huter EN, Shevach EM. Engagement of TLR2 Does not Reverse the Suppressor Function of Mouse Regulatory T Cells, but Promotes Their Survival. The Journal of Immunology. 2009; 183:4458–66. [PubMed: 19748987]
36. Newell EW, Sigal N, Bendall SC, Nolan GP, Davis MM. Cytometry by Time-of-Flight Shows Combinatorial Cytokine Expression and Virus-Specific Cell Niches within a Continuum of CD8+ T Cell Phenotypes. Immunity. 2012; 36:142–52. [PubMed: 22265676]
37. Betts MR, Nason MC, West SM, De Rosa SC, Migueles SA, Abraham J, et al. HIV nonprogressors preferentially maintain highly functional HIV-specific CD8+ T cells. Blood. 2006; 107:4781–9. [PubMed: 16467198]
38. Koh YT, Scatizzi JC, Gahan JD, Lawson BR, Baccala R, Pollard KM, et al. Role of Nucleic Acid-Sensing TLRs in Diverse Autoantibody Specificities and Anti-Nuclear Antibody-Producing B Cells. J Immunol. 2013; 190:4982–90. [PubMed: 23589617]
39. Guiducci C, Gong M, Cepika AM, Xu Z, Tripodo C, Bennett L, et al. RNA recognition by human TLR8 can lead to autoimmune inflammation. Journal of Experimental Medicine. 2013; 210:2903–19. [PubMed: 24277153]
40. Abujam B, Cheekatla S, Aggarwal A. Urinary CXCL-10/IP-10 and MCP-1 as markers to assess activity of lupus nephritis. Lupus. 2013; 22:614–23. [PubMed: 23629827]
41. Hasegawa H, Kohno M, Sasaki M, Inoue A, Ito MR, Terada M, et al. Antagonist of monocyte chemoattractant protein 1 ameliorates the initiation and progression of lupus nephritis and renal vasculitis in MRL/lpr mice. Arthritis & Rheumatism. 2003; 48:2555–66. [PubMed: 13130475]
42. Marks SD, Williams SJ, Tullus K, Sebire NJ. Glomerular expression of monocyte chemoattractant protein-1 is predictive of poor renal prognosis in paediatric lupus nephritis. Nephrology Dialysis Transplantation. 2008; 23:3521–6.
43. Kulkarni O, Pawar RD, Purschke W, Eulberg D, Selve N, Buchner K, et al. Spiegelmer Inhibition of CCL2/MCP-1 Ameliorates Lupus Nephritis in MRL-(Fas)lpr Mice. Journal of the American Society of Nephrology. 2007; 18:2350–8. [PubMed: 17625118]
44. Rovin BH. Urine Chemokines as Biomarkers of Human Systemic Lupus Erythematosus Activity. Journal of the American Society of Nephrology. 2005; 16:467–73. [PubMed: 15601744]
45. Bekeredjian-Ding I, Jego G. Toll-like receptors - sentries in the B-cell response. Immunology. 2009; 128:311–23. [PubMed: 20067531]
46. Martinez J, Huang X, Yang Y. Direct TLR2 Signaling Is Critical for NK Cell Activation and Function in Response to Vaccinia Viral Infection. PLoS Pathog. 2010; 6:e1000811. [PubMed: 20300608]
47. Esin S, Counoupas C, Aulicino A, Brancatisano FL, Maisetta G, Bottai D, et al. Interaction of Mycobacterium tuberculosisCell Wall Components with the Human Natural Killer Cell Receptors NKp44 and Toll-Like Receptor 2. Scand J Immunol. 2013; 77:460–9. [PubMed: 23578092]
48. Marcenaro E, Ferranti B, Falco M, Moretta L, Moretta A. Human NK cells directly recognize Mycobacterium bovis via TLR2 and acquire the ability to kill monocyte-derived DC. International Immunology. 2008; 20:1155–67. [PubMed: 18596023]
49. Lancioni CL, Li Q, Thomas JJ, Ding X, Thiel B, Drage MG, et al. Mycobacterium tuberculosis Lipoproteins Directly Regulate Human Memory CD4+ T Cell Activation via Toll-Like Receptors 1 and 2. Infection and Immunity. 2011; 79:663–73. [PubMed: 21078852]
50. Shireman PK, Contreras-Shannon V, Ochoa O, Karia BP, Michalek JE, McManus LM. MCP-1 deficiency causes altered inflammation with impaired skeletal muscle regeneration. Journal of Leukocyte Biology. 2006; 81:775–85. [PubMed: 17135576]
51. Kim RY, Hoffman AS, Itoh N, Ao Y, Spence R, Sofroniew MV, et al. Astrocyte CCL2 sustains immune cell infiltration in chronic experimental autoimmune encephalomyelitis. Journal of Neuroimmunology. 2014:1–9.

52. Atamas SP, White B. The role of chemokines in the pathogenesis of scleroderma. Curr Opin Rheumatol. 2003; 15:772–7. [PubMed: 14569209]

53. Brenner M, Laragione T, Gulko PS. Analyses of synovial tissues from arthritic and protected congenic rat strains reveal a new core set of genes associated with disease severity. Physiological Genomics. 2013; 45:1109–22. [PubMed: 24046282]

54. Bauer JW, Baechler EC, Petri M, Batliwalla FM, Crawford D, Ortmann WA, et al. Elevated serum levels of interferon-regulated chemokines are biomarkers for active human systemic lupus erythematosus. PLoS Med. 2006; 3:e491. [PubMed: 17177599]

55. Pascual V, Allantaz F, Patel P, Palucka AK, Chaussabel D, Banchereau J. How the study of children with rheumatic diseases identified interferon-α and interleukin-1 as novel therapeutic targets. Immunological Reviews. 2008; 223:39–59. [PubMed: 18613829]

56. O'Gorman WE, Huang H, Wei Y- L, Davis KL, Leipold MD, Bendall SC, et al. The Split Virus Influenza Vaccine rapidly activates immune cells through Fcγ receptors. Vaccine. 2014; 32:5989–97. [PubMed: 25203448]

57. Lundberg AM, Drexler SK, Monaco O, Williams LM, Sacre SM, Feldmann M, Foxwell BM. Key differences in TLR3/poly I:C signaling and cytokine induction by human primary cells: a phenomenon absent from murine cell systems. Blood. 2007; 110:3245–3252. [PubMed: 17660379]

KEY MESSAGES

1. Mass cytometry analysis demonstrates conserved cell type- and receptor-specific TLR activation signatures in healthy donors
2. Application of this systems scale approach to interrogate inflammatory disease reveals an altered monocytic chemokine signature in SLE

CAPSULE SUMMARY

Mass cytometry analysis of human TLR activation provides a comprehensive reference framework that can be applied to interrogate inflammatory processes, with the potential to identify candidate disease biomarkers and/or therapeutic targets.

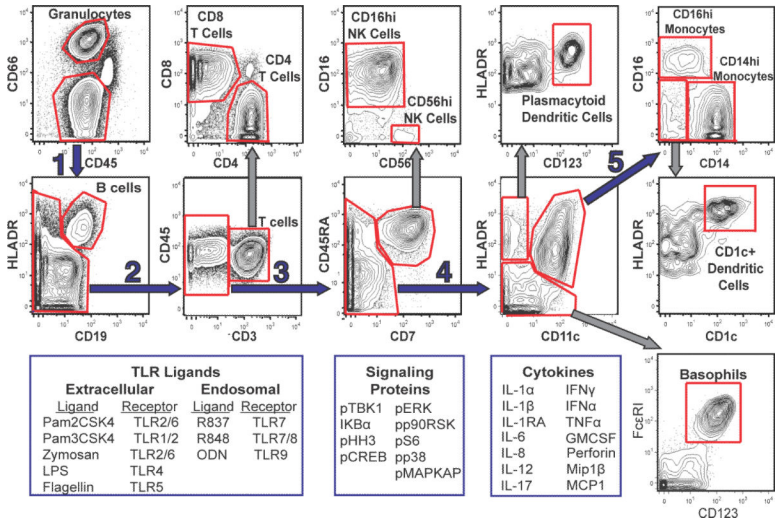

Figure 1. Mass cytometry identifies major immune cell subsets in human whole blood

Following fixation and RBC lysis, cells were labeled with 22 surface markers that defined 11 general cell types. Extended T cell gating strategy is shown in **Figure E1**. Subsequently, cells were permeabilized, stained with monoclonal antibodies that probe intracellular proteins (**Table E3**), and analyzed via mass cytometry. Representative data from one healthy donor is shown.

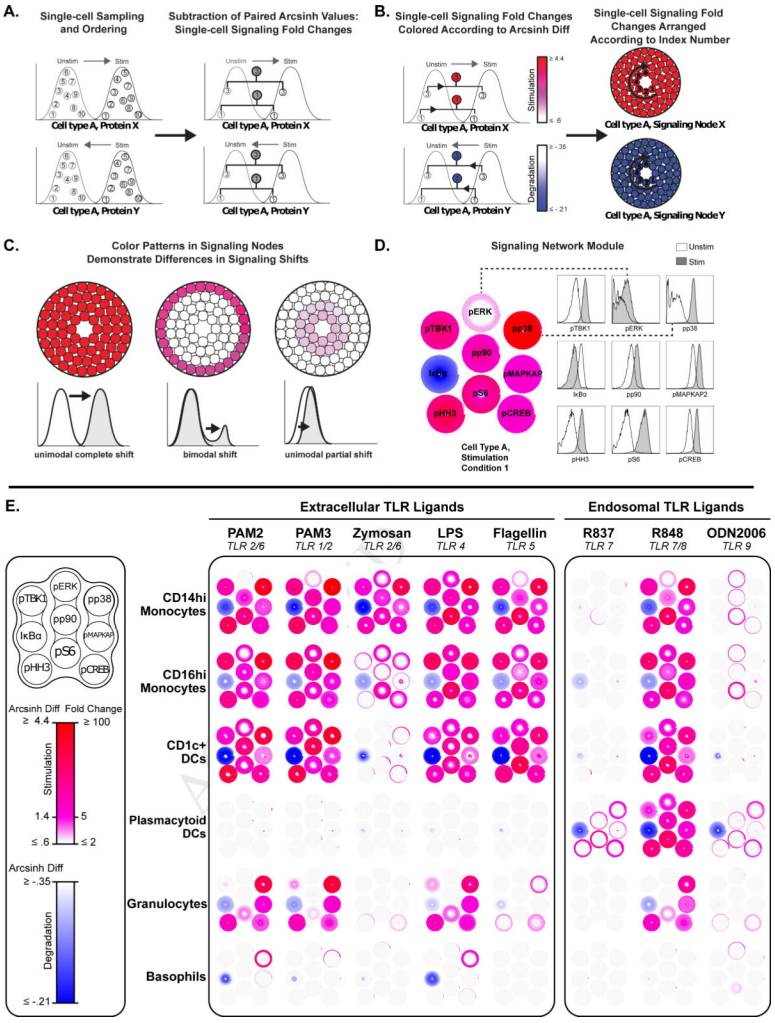

Figure 2. A signaling network heatmap visualization tool provides an integrated view of TLR signaling patterns

(**A**) Up to 1,000 representative cells were sampled for each cell type population, for unstimulated (unstim) and stimulated (stim) conditions. Cells were ordered from lowest to highest arcsinh transformed value for each signaling protein. Corresponding single-cell arcsinh values between unstim and stim cells were subtracted on a pair-wise basis, which constitute single-cell signaling fold changes. These single-cell signaling fold changes are indexed in the same numbered order as the cells from which they were derived, and (**B**) colored in red (phosphorylation) or blue (protein degradation) according to their arcsinh difference value. Single-cell signaling fold changes are arranged according to their index number, from lowest to highest, starting from the inside and moving clockwise to form a signaling node. (**C**) Signaling nodes demonstrate the distribution of responsive cells in a given population. The center of the node corresponds to the lowest values of the histograms, and the periphery corresponds to the highest values. Model activation patterns are shown. (**D**) Signaling nodes are organized in a “signaling network module,” reflecting a generalized structure of TLR response pathways. (**E**) Human whole blood was stimulated with TLR ligands indicated in **Figure 1** tables. Following stimulation cells were fixed, stained,

analyzed, and classified as described in **Figure 1**. Single-cell signaling fold changes were derived and organized as described above. Signaling data from one healthy donor is shown; additional donors and variances from other sampled donors are shown in **Figures E2** and **E3**.

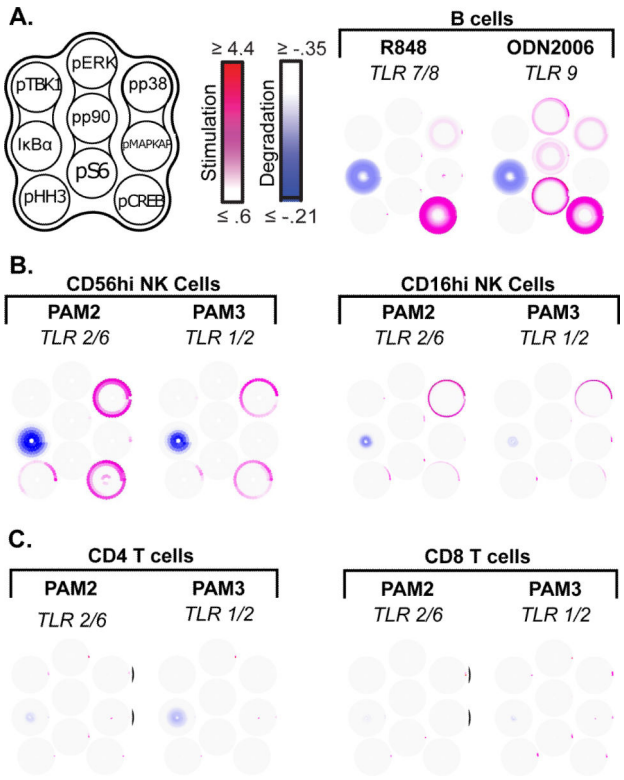

Figure 3. Signaling network heatmap demonstrates selective NF-κB activation in subsets of NK and T cells

(**A**) B cells respond to endosomal stimuli with induction of NF-κB pathway and CREB phosphorylation. Trace populations of (**B**) NK cells and (**C**) T cells responded to PAM2 and PAM3, with induction of NF-κB pathway. Representative data from one healthy donor is shown. For complete lymphoid single-cell heatmap, see **Figure E4**. For additional experiments involving purified NK and T cell populations, and their TLR2 responses from additional donors, see **Figures E5, E6, and E7**.

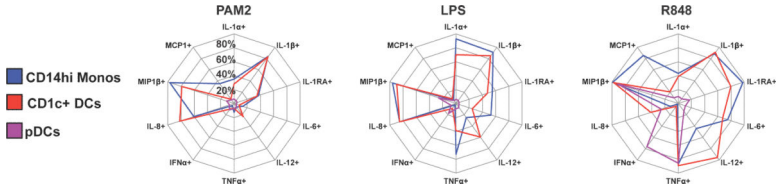

Figure 4. TLR-induced cytokine signatures demonstrate TLR agonist and cell type specificity

Human whole blood was stimulated with PAM2, LPS, and R848 for six hours in the presence of protein secretion inhibitors. Monocytes and dendritic cells were identified as indicated in **Figure 1**. Cells demonstrating cytokine production levels higher than the 95th percentile of unstimulated cells were defined as cytokine positive (**Figure E8**). Cytokine signatures are presented as radar plots with 20% radial intervals. Cytokines are arranged in functional families: IL1 family (IL-1α, IL-1β, IL1-RA), pro-inflammatory (IL-6, IL-12, TNFα, IFNα), and chemokines (Mip1β, MCP1, IL-8), in clockwise order. Average values based on responses from nine healthy donors are shown (cytokine variance data in **Figure E11**).

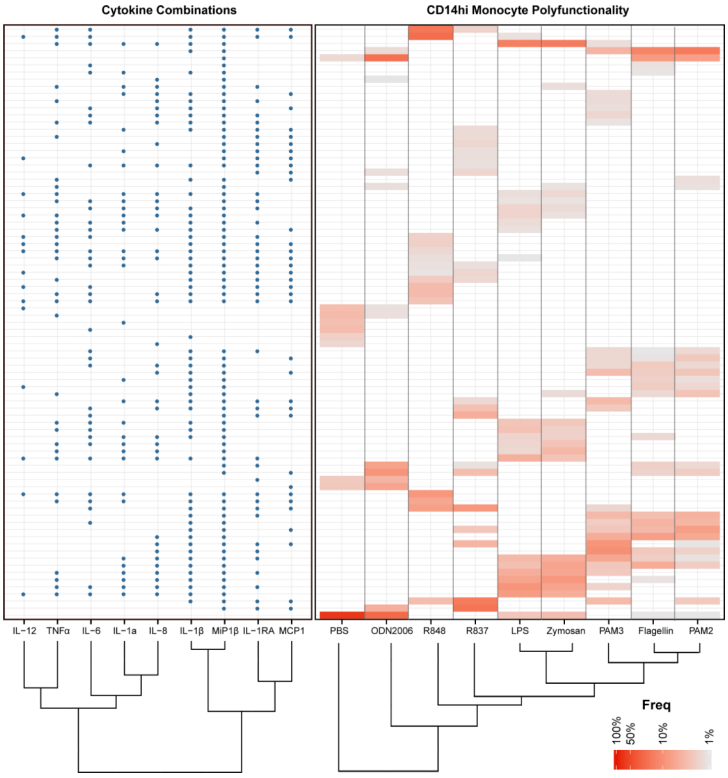

Figure 5. TLR ligands induce diverse combinatorial cytokine signatures in CD14hi monocytes

CD14hi monocyte combinatorial cytokine polyfunctionality was assessed in response to eight TLR ligands listed in **Figure 1** table. A Boolean gating script was used to quantify subgroup frequency based on a 95th percentile threshold (**Figure E8**). Cytokine combinations are represented as rows on the left panel, with blue dots indicating positivity for a particular cytokine. For a nine-cytokine analysis, 512 possible combinations of co-expressed cytokines are possible. Only cytokine combinations expressed by more than 1% of cells are depicted; 83 different cytokine combinations were detected at this level and above. Red color scaling indicates the frequency of each CD14hi monocyte subpopulation. Hierarchical clustering of cytokines and TLR ligands relate cytokine co-expression patterns (left panel), and cytokine combination patterns shared between TLR ligands (right panel), respectively. Data from one healthy donor is shown.

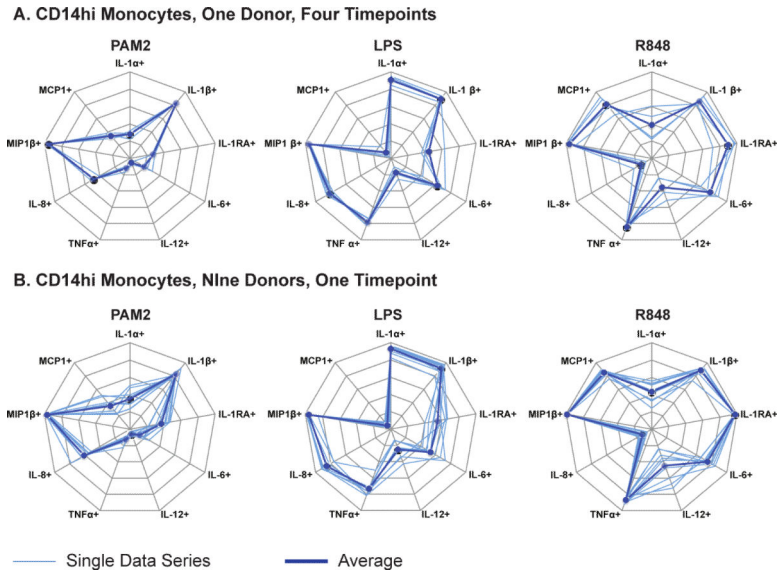

Figure 6. Intra- and inter-individual reproducibility of TLR-induced cytokine signatures in healthy donor CD14hi monocytes

(**A**) Thin lines relate longitudinal monthly blood draw samples for one healthy donor. Bold lines relate the average of all four samples. (**B**) Thin lines are specific to each distinct healthy donor. Bold lines represent the average of all nine healthy donor cytokine responses.

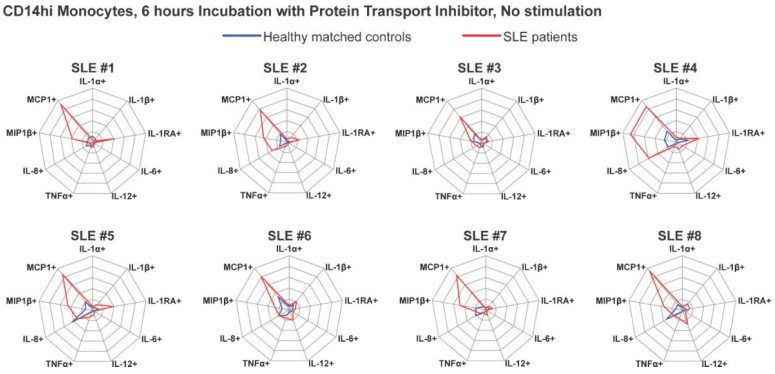

Figure 7. CD14hi monocytes from SLE patients show an inflammatory chemokine signature typified by MCP1

Cytokine positivity was defined based on the 95th percentile threshold of blood processed immediately after draw (time zero), and thus were internally controlled. Each radar plot represents the CD14hi monocytic cytokine signature of an SLE patient (red line) vs. healthy gender-matched control (blue line), after six-hour incubation period with protein secretion inhibitor (no exogenous stimuli).